Materials Letters 420 (2026) 140982

Contents lists available at ScienceDirect

Materials Letters

journal homepage: www.elsevier.com/locate/matlet

# Isothermal fatigue-induced precipitation in high-chromium ferritic steel: A microstructural analysis

Patrick Lehner [a], Michael Eusterholz [b,c], Ali Ahmadian [c,d], Tilmann Beck [a], Bastian Blinn [a,*]

[a] Institute of Materials Science and Engineering, RPTU, Kaiserslautern, Germany
[b] Institute of Applied Materials (IAM-WK), Karlsruhe Institute of Technology, Germany
[c] Karlsruhe Nano Micro Facility (KNMFi), Karlsruhe Institute of Technology, Germany
[d] Helmholtz Institute Ulm for Electrochemical Energy Storage, Karlsruhe Institute of Technology, Germany

ARTICLE INFO

*Keywords:*
HiperFer
Laves phase
APT
TEM

ABSTRACT

HiperFer-steels exhibit thermo-mechanically triggered Laves phase precipitation, leading to cyclic hardening during high-temperature fatigue. Thereby, particle-free zones (PFZ) at grain boundaries are formed, which act as crack initiation sites. At higher load amplitudes, the widths of these PFZ become smaller. To understand the underlying mechanism, high-resolution microstructural analyses were performed in this work, showing that in the PFZ a very low dislocation density is present, while the adjacent regions show a high dislocation density. It is assumed that the Laves phase-forming elements diffuse from interior grain regions to the PFZ and use the dislocations at the boundary between precipitation front and PFZ to form Laves phase particles. Thus, the PFZ become smaller with increasing plastic deformation, while no increase in dislocation density occurs.

## 1. Introduction

Energy transformation increases the relevance of fatigue and oxidation for steam power plants, where martensitic-ferritic 9% Cr-steels are used [1]. These steels show an insufficient corrosion resistance above 620 °C [2] and higher Cr-contents lead to undesired intermetallic phases, which reduce the high-temperature strength [3]. Thus, high-Cr ferritic steels (>15 wt% Cr) like HiperFer (High performance Ferrite) have gained attention [4,5]. HiperFer-steels are strengthened via Laves phase precipitates, increasing creep and thermomechanical fatigue strength [4,5]. The structure of Laves phase influences the strength [4,6] and can be tailored by plastic deformation combined with high temperatures [4,7].

In previous own work on a HiperFer-17Cr2, isothermal fatigue tests were performed in the Low Cycle (LCF, 0.05 Hz) and High Cycle Fatigue (HCF, 5 Hz) regime [6–8]. In the LCF-regime, a higher fatigue strength was observed [7,8], which is attributed to the extended loading time at low frequency, promoting Laves phase precipitation before severe damage accumulated [7]. For both frequencies, particle-free zones (PFZ) in the vicinity of grain boundaries (GB), which did not show any Laves phase precipitates, were observed [6,7]. Note that the PFZ act as crack initiation sites [4,9]. Consequently, it is required to understand the mechanism of PFZ formation. In previous work, it was assumed that the PFZ result from a segregation of Laves phase-forming elements (LPE: W, Nb, Si) at the GB during the prior heat treatment [10], which leads to a local depletion of LPE, disabling Laves phase precipitation. Note that the PFZ-width $w_{PFZ}$ decreased during LCF-loadings but remained unchanged during HCF-loadings after they occurred [6]. In previous work this reduction in $w_{PFZ}$ was attributed to higher dislocation densities caused by LCF-loadings, promoting pipe diffusion of LPE from intragranular regions to the PFZ [6,7], which enables Laves phase precipitation. However, the underlying mechanism for the difference in evolution of $w_{PFZ}$ remained uncertain, being objective of this work.

## 2. Material and methods

The investigated specimens of HiperFer-17Cr2 (details in [6–8]) were extracted from hot-rolled sheets and subsequently recrystallized (1050 °C, 15 min, air cooling), followed by two annealing steps (545 °C/5 h and 650 °C/1 h, each followed by water quenching).

The microstructural analyses were performed on specimens isothermally fatigued at 635 °C and were focused on two differently loaded conditions and the initial state. The loaded specimens were fatigued with the setup described in [6–8] to half of the lifetime expected from previous work [8], i.e., 2000 cycles at a stress amplitude $\sigma_a$ = 260 MPa (LCF-loading at 0.05 Hz) and 20,000 cycles at $\sigma_a$ = 210 MPa

* Corresponding author.
*E-mail address:* b.blinn@mv.rptu.de (B. Blinn).

https://doi.org/10.1016/j.matlet.2026.140982
Received 7 April 2026; Received in revised form 13 May 2026; Accepted 24 May 2026
Available online 25 May 2026

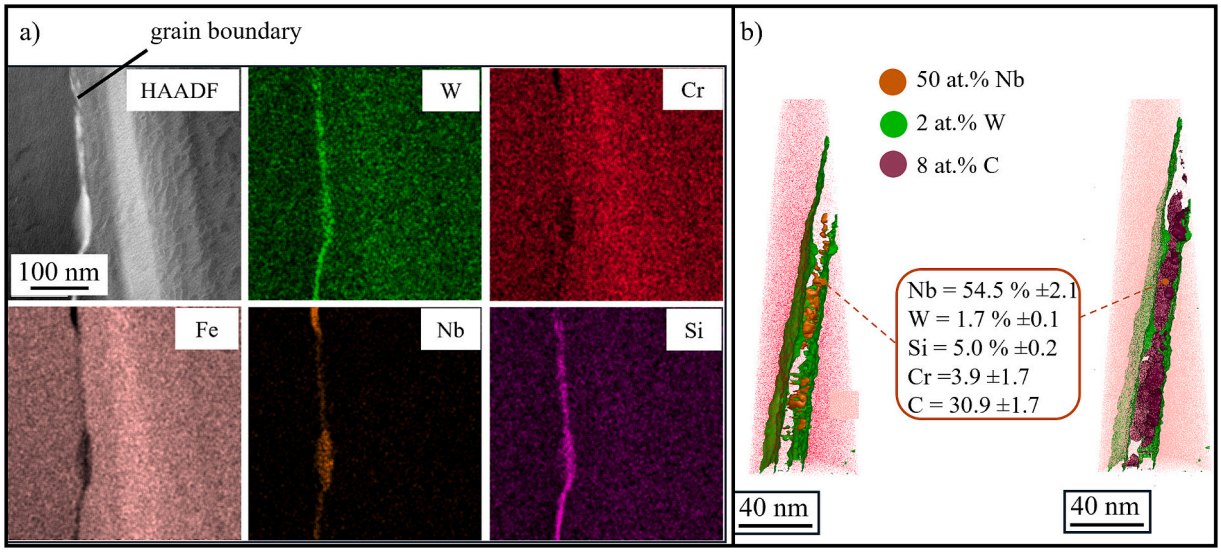


**Fig. 1.** Distribution of elements at a GB in the initial state determined via (a) STEM-EDX and (b) APT (contents in at.%).

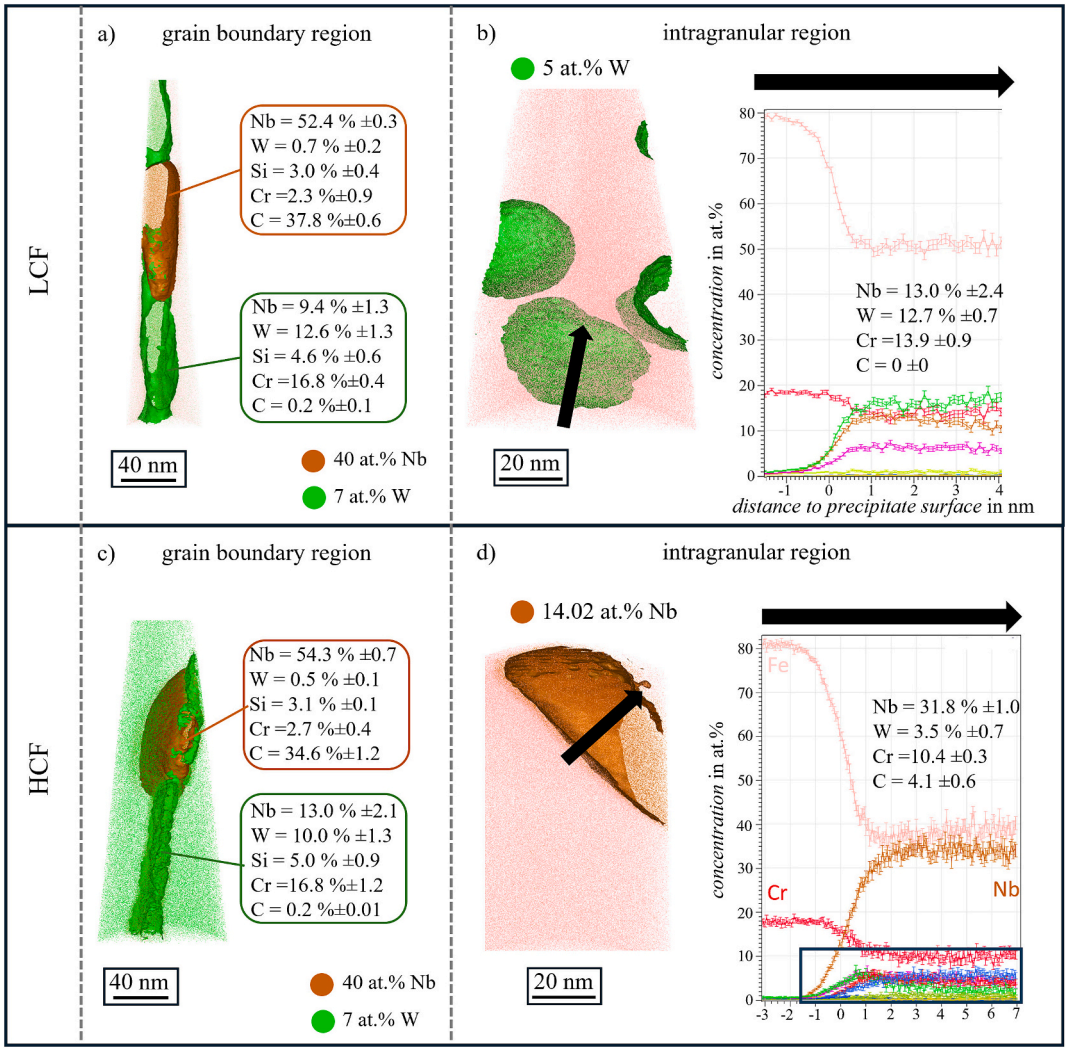


**Fig. 2.** APT analyses of GB and intragranular regions in specimens subjected to LCF- and HCF-loading (concentrations in at.%).

(HCF-loading at 5 Hz).

For analysis of the Laves phases and PFZ, sections of the specimens' gauge lengths were etched with 5%-$H_2SO_4$. Electron-transparent samples for TEM (Transmission Electron Microscopy) and APT (Atom Probe

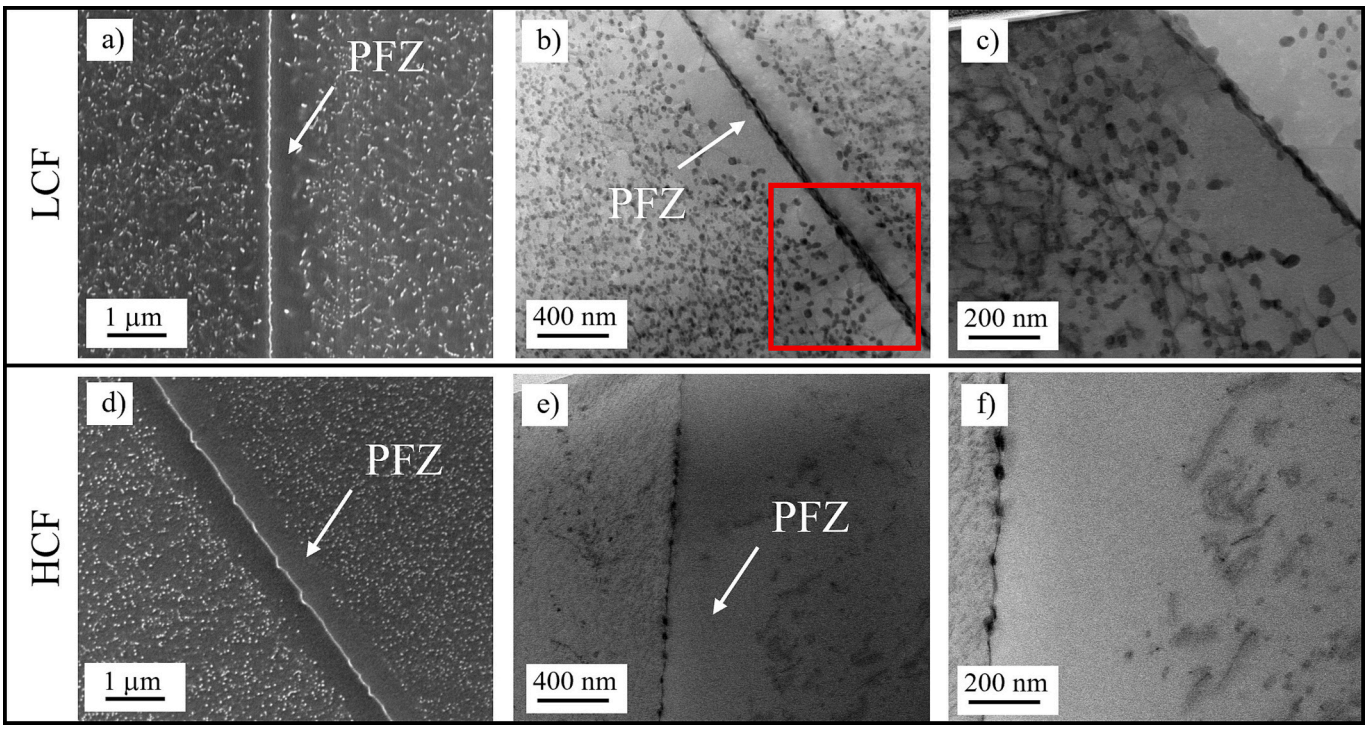


**Fig. 3.** Images of PFZ formed after LCF- and HCF-loading obtained by (a and d) SEM and (b-c and e-f) ABF-STEM.

Tomography) analyses were extracted via standard lift-out procedure, using a Strata 400 dual-beam scanning electron microscope (SEM) equipped with a focused ion beam system of Thermo Fisher Scientific. For both fatigued conditions, regions at the GB and within the grains were investigated. Moreover, the GB region of the initial state was analyzed. The TEM analyses were performed using an aberration-corrected Themis 300 microscope equipped with a ChemiSTEM SuperX energy dispersive X-ray spectroscopy (EDX) detector. For scanning TEM (STEM), high-angle annular dark-field (HAADF) and annular bright-field (ABF) modes were used at a camera length of 100 mm, while an acceleration voltage of 300 kV and a probe current of 80pA were utilized. The data were analyzed using Velox 3.13.0 software from Thermo Fisher Scientific. APT analyses were performed on a LEAP 4000× HR in pulsed laser mode (355 nm wavelength, 40pJ pulse energy, 200 kHz repetition rate) at a base temperature of 40 K and a detection rate of 0.005 ions per pulse, while data were analyzed using AP Suite 6.3.1 (Cameca).

## 3. Results and discussion

As shown in Fig. 1, the initial state exhibits an enrichment of W, Nb and Si at the GB, but no Laves phases precipitates (Fig. 1b). The APT analysis confirms the solution of W and Nb, i.e., the key LPE in HiperFer-17Cr2, at the GB, while Nb carbides are detected by elevated Nb and C contents.

APT analyses at the fatigued conditions (Fig. 2) show coarsening of the Nb carbides at the GB after both LCF- and HCF-loading. Moreover, Laves phases form at the GB, with roughly similar contents of Nb and W between both conditions. The elemental distributions (Fig. 2a and c) indicate high-temperature Laves phases with a relatively high W content [11,12], requiring higher temperatures and/or time for diffusion, since W has a lower diffusivity [13]. This Laves phase formation might lead to wetting of the GB by secondary solid phase [14] (Fig. 3 b-f), which influences the mechanical properties [15]. Note that the Laves phase precipitation at the GB, and hence the fraction of completely wetted GB is more pronounced after LCF-loading, presumably contributing to the differences observed in fatigue behavior.

For both loading conditions, intragranular Laves phase precipitation is observed (Fig. 2b and d). While for the LCF condition the intragranular Laves phases have a similar chemical composition as the particles observed at the GB, the intragranular precipitates observed after HCF-loading exhibit higher Nb and lower W fractions, indicating low-temperature Laves phases [11,12]. This is attributed to the shorter loading time at HCF- than LCF-loading (4000 s vs. 40,000 s), limiting W diffusion. Thus, the different chemical composition of the intragranular Laves phases might influence the mechanical properties [6]. As the GB shows a locally increased W content in the initial state, the high-temperature Laves phase forms there even during the shorter HCF-loading.

Complementary (S)TEM analyses of GB regions in the loaded conditions (Fig. 3) confirm the absence of Laves phases in the PFZ, consistent with the local depletion of LPE in the vicinity of the GB (Fig. 1). Moreover, the (S)TEM images in Fig. 3 reveal that the PFZ are nearly dislocation-free after HCF- and LCF-loading. However, in the regions adjacent to the PFZ, a high number of dislocations is present between the Laves phases, with a higher dislocation density in the LCF- than in the HCF-condition. Hence, a significantly lower dislocation density in the PFZ in relation to their adjacent regions can be concluded.

Previous work [6] suggested that pipe diffusion along dislocations reduces $w_{PFZ}$ during LCF-loading due to high dislocation density, enabling the transport of LPE from the grain interior to the PFZ, where they precipitate at existing dislocations. Although this hypothesis is supported by the ABF-STEM images (Fig. 3), the very low dislocation density in PFZ was unexpected. The TEM investigations suggest that Laves phase particles form at dislocations between the PFZ and the precipitation front, thereby reducing $w_{PFZ}$. For this, sufficient contents of LPE are required. Since the PFZ is depleted of these elements, a diffusion of LPE from the grain interior towards the PFZ is a prerequisite. This is enhanced by pipe diffusion, being more pronounced in LCF condition due to higher dislocation density. Due to the formation of precipitates at dislocations, the latter are pinned, resulting in a low dislocation density in PFZ.

Note that the $w_{PFZ}$ reduction may also occur under HCF-loadings but is less pronounced due to lower plastic deformation and higher

frequency. The resulting lower dislocation density reduces pipe diffusion and hence the supply of LPE. Moreover, the faster local plastic deformation enhances damage accumulation in the PFZ, leading to failure before a reduction of $w_{PFZ}$ occurs.

The proposed mechanism is supported by additional experiments [7]: a specimen fatigued at HCF-loading ($\sigma_a$ = 210 MPa, 5 Hz, 635 °C) and subsequently aged at 635 °C for 110 h, being equivalent to LCF-loading time, showed no change in $w_{PFZ}$. In contrast, continuous LCF-loading with the same $\sigma_a$ at 0.05 Hz resulted in a progressive $w_{PFZ}$ reduction, indicating that thermally induced diffusion alone is insufficient for $w_{PFZ}$ reduction. This demonstrates that $w_{PFZ}$ reduction in HiperFer-17Cr2 requires both continuous dislocation motion into the PFZ and availability of LPE (Nb, W).

Note that the marked region in Fig. 3b suggests that connections between the GB and precipitation front by dislocations may enable pipe diffusion of LPE from intragranular regions to the GB, since coarsening of the Laves phase particles is visible there. However, this needs to be verified in future work.

## 4. Conclusion

APT and TEM analyses revealed an initial enrichment of LPE and Nb carbides at grain boundaries in HiperFer-17Cr2. During fatigue loading, Laves phase precipitation occurs at grain boundaries and within grains, accompanied by coarsening of Nb carbides. Enabled by a longer loading time, which promotes diffusion processes, LCF-loading results in Laves phases with higher W content compared to HCF-loading. The reduction in $w_{PFZ}$ is attributed to increased plastic deformation at LCF-loadings, leading to higher dislocation densities, and therewith more nucleation sites as well as enhanced pipe diffusion of Nb and W. Both are prerequisites for Laves phase precipitation in the PFZ, progressively reducing the $w_{PFZ}$.

## CRediT authorship contribution statement

**Patrick Lehner:** Writing – original draft, Visualization, Methodology, Conceptualization. **Michael Eusterholz:** Writing – review & editing, Visualization, Methodology, Investigation, Conceptualization. **Ali Ahmadian:** Writing – review & editing, Visualization, Methodology, Investigation. **Tilmann Beck:** Writing – review & editing, Supervision, Resources. **Bastian Blinn:** Writing – original draft, Visualization, Supervision, Conceptualization.

## Declaration of competing interest

The authors declare that they have no known competing financial interests or personal relationships that could have appeared to influence the work reported in this paper.

## Acknowledgement

The authors thank the DFG for the financial support (project number: 450763904). This work was carried out with the support of the Karlsruhe Nano Micro Facility (KNMFi), an Open Access Research Infrastructure within the Karlsruhe High Technology Hub at the Karlsruhe Institute of Technology (KIT – The University in the Helmholtz Association).

## Data availability

Data will be made available on request.

## References

[1] A. Kumar, C. Pandey, Int. J. Press. Vessel. Pip. 198 (2022) 104678, https://doi.org/10.1016/j.ijpvp.2022.104678.
[2] S. Sorrentino, Elsevier, 2017, pp. 247–319, https://doi.org/10.1016/B978-0-08-100552-1.00009-9.
[3] F. Abe, J. Press. Vessel. Technol. 138 (2016) 040804, https://doi.org/10.1115/1.4032372.
[4] B. Kuhn, et al., Metals 10 (2020) 463, https://doi.org/10.3390/met10040463.
[5] B. Kuhn, M. Talik, Proc. 10th Liége Conf. Mater. Adv. Power Eng, 2014, pp. 264–273.
[6] P. Lehner, et al., Mater. Sci. Eng. A 923 (2025) 147713, https://doi.org/10.1016/j.msea.2024.147713.
[7] P. Lehner, et al., Mater. Sci. Eng. A 948 (2025) 149330, https://doi.org/10.1016/j.msea.2025.149330.
[8] P. Lehner, et al., Int. J. Fatigue 186 (2024) 108388, https://doi.org/10.1016/j.ijfatigue.2024.108388.
[9] J. Lopez Barrilao, et al., Micron 108 (2018) 11–18, https://doi.org/10.1016/j.micron.2018.02.008.
[10] X. Fan, et al., Appl. Sci. 10 (2020) 5713, https://doi.org/10.3390/app10165713.
[11] J. Lopez Barrilao, et al., Mater. Sci. Technol. 33 (2017) 1056–1064, https://doi.org/10.1080/02670836.2016.1244039.
[12] J. Lopez Barrilao, et al., Micron 101 (2017) 221–231, https://doi.org/10.1016/j.micron.2017.07.010.
[13] J. Pöpperlová, et al., Appl. Sci. 10 (2020) 4472, https://doi.org/10.3390/app10134472.
[14] B. Straumal, et al., J. Mater. Sci. 60 (2025) 20603–20616, https://doi.org/10.1007/s10853-025-10818-5.
[15] A. Kilmametov, et al., Mater. Lett. 406 (2026) 139950, https://doi.org/10.1016/j.matlet.2025.139950.